

Article

PLA Films Containing Montmorillonite Nanoclay–Citronella Essential Oil Hybrids for Potential Active Film Formulation

Rafaela R. Ferreira ^{1,*}, Marilia C. Farina ², Anderson Maia ² and Rondes F. S. Torin ^{2,*} 

¹ Center for Engineering, Modeling, and Applied Social Sciences—CECS, Federal University of ABC (UFABC), Santo André 09210-580, SP, Brazil

² Centro Estadual de Educação Tecnológica Paula Souza—Faculdade de Tecnologia de Mauá (FATEC MAUÁ), Mauá 09390-120, SP, Brazil

* Correspondence: rafaela_reisf@hotmail.com (R.R.F.); rondes.torin@fatec.sp.gov.br (R.F.S.T.)

Abstract: This work evaluated the synergistic effect of citronella essential oil (Ct) and montmorillonite (MMT) (called hybrid compound) incorporated in Poly(lactic acid) (PLA) films at different concentrations (3, 10, 15, and 20 wt%). PLA films were characterized using X-ray diffraction, SEM, TGA, and DSC considering their mechanical properties and essential oil migration. XRD analysis showed the effective interaction between MMT and oil. Thermal analysis, SEM, and mechanical tests were essential to understand the saturation point of the PLA composites. Samples with 15% and 20% of Ct showed a crystallinity reduction of 0.5% compared to samples with 3% and 10% of Ct. PLA/MMT–Ct showed a reduction in tensile strength of the order of 16 and 24, correlated to 15% and 20% of the Ct content, respectively, compared to PLA/MMT–Ct3%. Migration tests showed fast oil delivery correlated with high oil concentration, as evidenced using the PLA/MMT–Ct20% sample results, which showed an estimated release of 50% in the first 150 h due to system saturation, and the remaining being released in the last 350 h. Therefore, the migration tests provide an effective Ct concentration range promising for application with active packaging due to the intrinsic antimicrobial properties of Ct.

Keywords: poly(lactic acid); nanoclay; essential oil; film



Citation: Ferreira, R.R.; Farina, M.C.; Maia, A.; Torin, R.F.S. PLA Films Containing Montmorillonite Nanoclay–Citronella Essential Oil Hybrids for Potential Active Film Formulation. *Macromol* **2023**, *3*, 200–210. <https://doi.org/10.3390/macromol3020012>

Academic Editor: Dimitrios Bikiaris

Received: 2 November 2022

Revised: 3 May 2023

Accepted: 5 May 2023

Published: 8 May 2023



Copyright: © 2023 by the authors. Licensee MDPI, Basel, Switzerland. This article is an open access article distributed under the terms and conditions of the Creative Commons Attribution (CC BY) license (<https://creativecommons.org/licenses/by/4.0/>).

1. Introduction

Polymeric materials from fossil sources are broadly used due to their properties and cost [1]. However, these polymers have non-biodegradable properties and may cause environmental problems such as increased carbon dioxide (CO₂) production and depletion of fossil resources [2]. Because of this scenario, several efforts are being made to reduce its consumption, and an alternative is using renewable polymeric materials based on environmentally friendly sources [3].

Poly(lactic acid) (PLA) is one of the most popular, eco-friendly, compostable degraded, biocompatible, and bio-based polyesters [4]. It has been extensively investigated in the literature due to its numerous potential advantages, such as good processability, biocompatibility, and physical properties, including high strength, stiffness, rigidity, clarity, and recyclability [5]. However, brittleness, poor elongation at break, inferior barrier behavior, restricted processability, and low melt strength are some of the challenges associated with PLA, significantly limiting its application as a flexible packaging film [6,7]. To overcome these limitations, PLA matrix blends with nanofillers/reinforcements enabling the formation of nanocomposites is by far the most accessible and most efficient approach for modifying and improving the properties of PLA and expanding its end-use application fields [8,9]. In this context, the literature has extensively investigated nanocomposite formulations that offer significant improvements in PLA properties [10,11].

Montmorillonite nano clay (MMT) are compounds that contain at least one dimension on a nanometric scale, presenting two types of reticulated structures: fibrous and lamellar

phyllosilicates [12]. Incorporating nano clay into a polymeric matrix offers some challenges associated with its degree of dispersion and homogeneity. In this sense, the incorporation of lamellar nanofillers with high aspect ratio, such as montmorillonites, has significantly enhanced mechanical, gas barrier, and optical properties of the polymer matrix [13]. MMT is formed by a gibbsite octahedra layer between two silica tetrahedra layers. This type of nano-clay has the characteristic of having water molecules between its structural units. For this reason, it normally has a hydrophilic character; therefore, for a good dispersion in polymeric matrices, it must become organophilic [12]. The organophilization of MMT provides expansion between the gaps that facilitate the incorporation of polymeric chains, also characterizing the carrier property of active ingredients [14]. A promising proposal is the incorporation of nano clay-essential oil (EO) hybrids in polymer films due to the clay's ability to assimilate EOs between its lamellae and act as a carrier [15], creating new materials with innovative characteristics that can be applied in the packaging sector.

Citronella EO (Ct) has citronella as its main compound, responsible for antioxidant properties [16] and antimicrobial properties [17]. However, EO has low solubility in water, organoleptic taste, and low thermal stability (i.e., high volatility) [18,19]. Due to its sensitivity to decomposition at high temperatures, the quest to prolong the EO release time and obtain a slow-release effect has been investigated.

In recent years, the creation of compostable biodegradable films has been a topic of interest as alternatives to conventional products are sought. In this sense, this study aimed to prepare PLA nanocomposites reinforced with the MMT-Ct hybrid at different concentrations, through the homogenization method, with the aim of developing active films. The films' morphological, thermal, and mechanical properties and their active properties were evaluated. The results indicate that the films obtained have potential application in the packaging sector as a sustainable alternative with advantageous properties.

2. Materials and Methods

2.1. Materials

Poly (lactic acid) (PLA) 7001D (with a specific gravity of 1.24 g cm^{-3} , and a melt flow index (MFI) of $6 \text{ g } 10 \text{ min}^{-1}$ ($210 \text{ }^\circ\text{C}$, 2.16 kg), Mw of $83,300 \text{ g/mol}$, and 1.5% of D-isomer, supplied by NatureWorks. Cloisite[®] 20A (montmorillonite (MMT) modified with bis (hydrogenated tallow alkyl) dimethyl ammonium) was supplied by Southern Clay Products, Inc. Tween 80 was purchased from Synth (São Paulo, Brazil). Citronella (Ct) essential oil was purchased from Ferquima (São Paulo, Brazil).

2.2. Methods

2.2.1. Hybrid Preparation

The hybrid (MMT-Ct) was developed based on the research of Torin et al. ¹⁵ Briefly, the MMT-Ct hybrid was prepared in mass ratios 1:2 of MMT (50 g) and Ct (100 g), which were added to a solution containing Tween 80 (10 g) and water (150 mL). The mixture was magnetically stirred at 800 rpm (Fisatom model 753A, São Paulo, Brazil) until complete homogenization. Then, it was dried (Digital drying oven, FANEM Ltd., São Paulo, Brazil) at $100 \text{ }^\circ\text{C}$ for 8 h.

2.2.2. Preparation of PLA/MMT-Ct Nanocomposites

Poly(lactic acid) (PLA) nanocomposites with different MMT-C contents (3, 10, 15, and 20% *w/w*) were prepared via melt mixing, using a high-speed homogenizer Drays K-mixer model MH-50H from MH Equipamentos Ltda (Guarulhos, Brazil). Then, the material was hot pressed, in a hydraulic press model BTC 9090, Marconi, at $160 \text{ }^\circ\text{C}$ and 4 tons, for 4 min to obtain 50μ thick films and then stored for analysis. The nomenclatures for the processed nanocomposites are presented in Table 1.

Table 1. Formulation of each nanocomposite prepared, considering the weight of PLA, MMT, and Ct (g).

| Samples | PLA (g) | MMT (g) | Ct (g) |
|---------------|---------|---------|--------|
| PLA | 100 | - | - |
| PLA/MMT-Ct3% | 100 | 1.0 | 2.0 |
| PLA/MMT-Ct10% | 100 | 3.7 | 7.4 |
| PLA/MMT-Ct15% | 100 | 5.8 | 11.7 |
| PLA/MMT-Ct20% | 100 | 8.3 | 16.6 |

2.3. Characterizations of Nanocomposites

2.3.1. X-ray Diffraction

X-ray diffraction data were collected on a D8 Focus diffractometer (Bruker AXS, Karlsruhe, Germany), operating at 40 kV and 40 mA, with monochromatic CuK α 1 radiation ($\lambda = 1.54056 \text{ \AA}$). Measurements were conducted in the following conditions: 0.01° step width, 100 s counting time at each 0.5° , and 2θ ranging from 10 to 40° . In addition, it was necessary to carry out a deconvolution analysis, and the OriginPro 8 2009 software was used for this.

Equation (1) was used to estimate the crystallinity index (CI) of PLA films by the ratio between the crystalline peaks areas (I_c) and the amorphous halo (I_a) [20].

$$CI = \frac{I_c}{I_c + I_a} * 100\% \quad (1)$$

2.3.2. Scanning Electron Microscopy

PLA nanocomposite samples were morphologically analyzed in a scanning electron microscope, model JCM-6000 (JEOL Ltd., Akishima, Tokyo, Japan), at 10 kV acceleration voltage. The samples were previously sputtered with gold with 20 nm thickness using a Leica EM ACE 200 (Leica Microsystems GmbH, Wetzlar, Germany) sputter coater.

2.3.3. Thermogravimetric Analysis

The thermogravimetric analysis evaluated the variation in membrane weight as a function of the progressive increase in temperature (30 – $600 \text{ }^\circ\text{C}$), time (heating rate of $10 \text{ }^\circ\text{C min}^{-1}$), and nitrogen atmosphere (N_2) with a flow of 50 mL min^{-1} . The STA 6000 (TA Instruments, New Castle, DE, USA) equipment was used. Data processing was performed with the support of Origin 8.0 software.

2.3.4. Differential Scanning Calorimetry

The calorimetric analyses were performed on a differential scanning calorimeter (DSC) from TA Instruments, Model Q-20. About 10.0 mg of each sample was packed in hermetically sealed aluminum crucibles. The samples underwent the heat/cool/heat test with temperatures between 80 to $180 \text{ }^\circ\text{C}$, with a heating rate of $10 \text{ }^\circ\text{C min}^{-1}$, under an inert nitrogen atmosphere (50 mL min^{-1}). The degree of crystallinity, X_c (%), was calculated from the area under the peak of the second heating sweep using the following Equation (2):

$$X_c(\%) = \frac{\Delta H_m}{\Delta H_{M\infty}} * 100 \quad (2)$$

where $\Delta H_{M\infty}$ is the experimental enthalpy of fusion, and ΔH_m is the theoretical enthalpy of 100% crystalline PLA; the latter assumes an estimated value of 93 J/g [21].

2.3.5. Mechanical Tests

Mechanical tests characterizing tensile properties were conducted to determine the nanocomposite strength in a Universal Machine Instron, 3367 model (Norwood, MA, USA). The tests were carried out according to ASTM D-638-14, comprising type IV, specified in the standard, with a test speed of 50 mm min^{-1} , and a load cell of 50 kN.

2.3.6. Migration Test

The procedure for performing the Migration Test was adapted from the ASTM C 772-0 standard. The dimensions of the specimens were 38 mm wide, 38 mm long, and 4 mm thick. The samples were placed between two filter papers of 76 mm in diameter in an oven provided with air circulation, with a temperature of 70 °C for three weeks, and in the last week of the test, the temperature was changed to 100 °C. Changes in sample masses were monitored within 24 h for 20 days.

3. Results

3.1. X-ray Diffraction

The influence of MMT nanoclay on the crystallinity of PLA was investigated via the XRD spectra of MMT neat in comparison to PLA pure and PLA/MMT-Ct, with different content of Ct, as shown in Figure 1. MMT neat exhibited characteristic XRD spectra; as shown in Figure 1A, we observed 2 θ peaks at approximately 6.0° and 15.5° corresponding to the crystallographic planes (001) and (003), respectively, which are characteristic of MMTs modified with the alkyl group [22]. Similar results were found by Torin and colleagues [15]. On the other hand, the PLA pattern presented characteristic peaks at 16.0° and 19.0° (2 θ) that are associated with the crystallographic plane (110), (200), and (203), respectively, according to the literature [23,24].

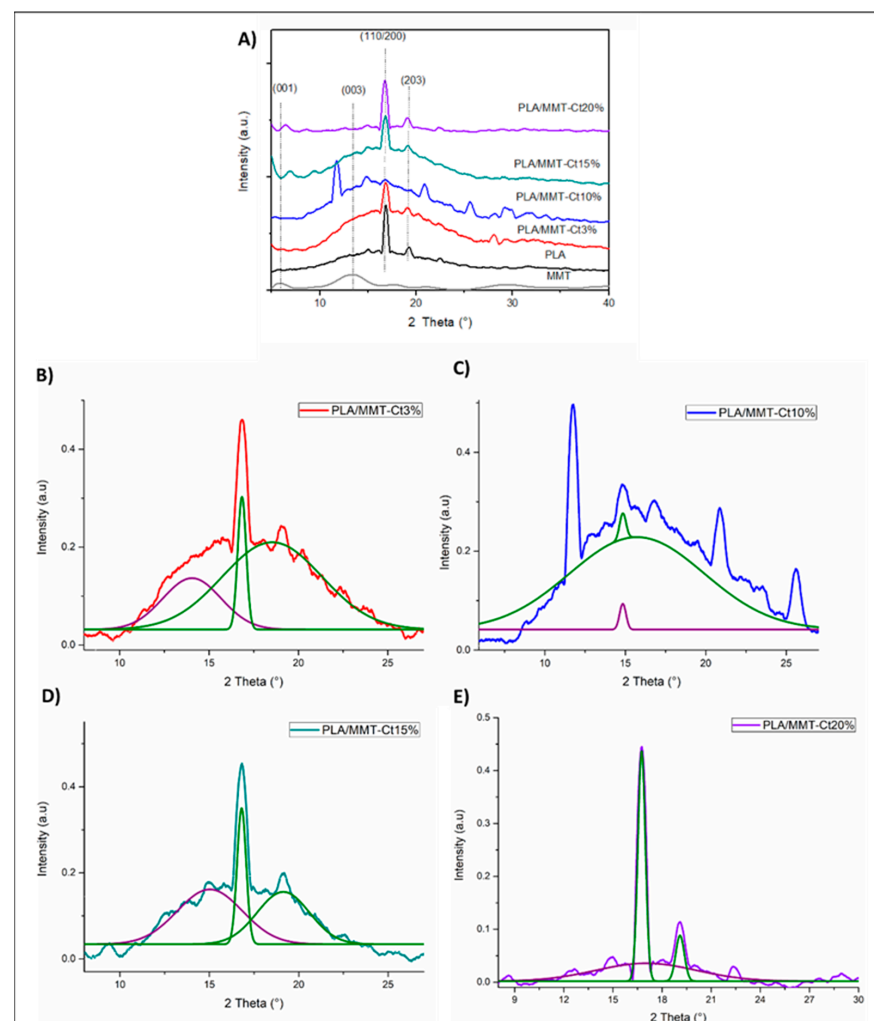


Figure 1. (A) XRD pattern of PLA samples and their PLA/MMT-Ct composites; XRD curves and their deconvolutions (B) PLA/MMT-Ct3%; (C) PLA/MMT-Ct10%; (D) PLA/MMT-Ct15% and (E) PLA/MMT-Ct20%.

The addition of MMT-Ct to the PLA caused, in all samples, a small baseline increase, which according to Rhim, may indicate a small intercalation of the PLA chains between the lamellas of the MMT nanoclay [22]. Thus, peak deconvolution was performed to understand the structure of the composites obtained, PLA/MMT-Ct. The results are shown in Figure 1B–E and clearly indicate significant changes when the MMT-Ct hybrid is added to the PLA. Similar results have been reported in the literature for polymeric composites with MMT, when MMT is added to the polymeric matrices and supports that polymeric chain intercalation occurs between the clay lamellas [25].

A decreasing crystallinity index (CI), as shown in Table 2, was observed in PLA films with the addition of MMT-Ct hybrids in different proportions: 83%, 80%, 73%, 69%, and 62% for PLA, PLA/MMT-Ct3%, PLA/MMT-Ct10%, PLA/MMT-Ct15%, and PLA/MMT-Ct20%, respectively. This effect can be attributed to the EO exudation of the MMT-Ct hybrid into the polymeric matrix, acting as a plasticizer and reducing the crystalline properties of the films. As the amount of hybrid in the PLA matrix increased, there was an increase in the amorphous character of the films, resulting in freer paths and facilitating the diffusion of EO from the MMT layers to the film surface.

Table 2. Crystallinity index (CI) of PLA films without or with hybrid MMT-Ct calculated by XRD, and TGA and DSC results of PLA and PLA/MMT-Ct.

| Samples | XRD | TGA | | DTG | DSC | | |
|---------------|--------|---------------------|---------------------|-----------------------|---------------------|---------------------|--------------------|
| | CI (%) | T ₁ (°C) | T _F (°C) | T _{MAX} (°C) | T _m (°C) | T _c (°C) | X _c (%) |
| PLA | 83 | 303.7 | 377.0 | 356.0 | 153.67 | 107.06 | 3.11 |
| PLA/MMT-Ct3% | 80 | 320.7 | 375.1 | 354.7 | 153.83 | 115.5 | 2.79 |
| PLA/MMT-Ct10% | 73 | 273.5 | 385.6 | 362.4 | 152.32 | 99.94 | 2.86 |
| PLA/MMT-Ct15% | 69 | 321.5 | 386.5 | 354.4 | 152.06 | 99.8 | 3.12 |
| PLA/MMT-Ct20% | 62 | 301.6 | 393.3 | 356.6 | 152.59 | 97.34 | 2.62 |

3.2. Scanning Electron Microscopy

Scanning electron microscopy (SEM) of the PLA and its composites were performed to obtain information about the influence of MMT and MMT-Ct hybrids on surface roughness and structure–property relationships. From the SEM images, as shown in Figure 2, it is possible to observe that the MMT-Ct contents lead directly to an increase in the roughness aspect, and the absence of domains, as agglomeration regions, suggests a homogeneous dispersion of MMT into the polymeric matrix. The influence of MMT on the roughness of polymeric matrix is expected according to the literature [25]. These results are consistent with those obtained on XRD, indicating a good dispersion between the PLA/MMT-Ct system. Shojaee-Aliabadi et al. observed a similar result, indicating smooth and continuous microstructure for the pure κ -carrageenan film and emulsified films [26].

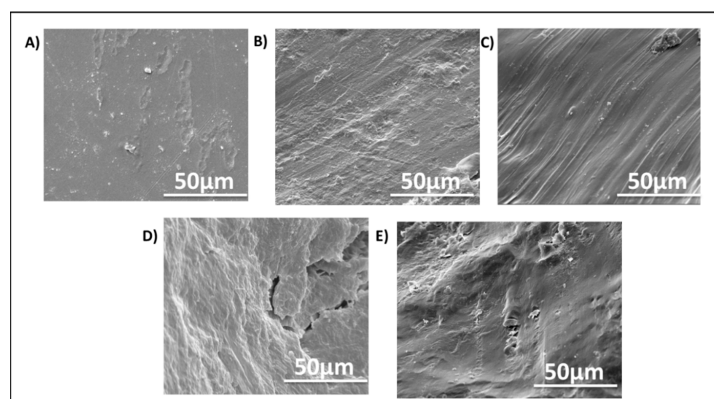


Figure 2. SEM micrographs of the standard sample and its composites (A) PLA; (B) PLA/MMT-Ct3%; (C) PLA/MMT-Ct10%; (D) PLA/MMT-Ct15%, and (E) PLA/MMT-Ct20%.

3.3. Thermogravimetric Analysis (TGA)

Thermal stability of the samples PLA and PLA with different contents of MMT–Ct hybrids were evaluated via TGA. Results obtained from TGA are shown in Figure 3A, and its derivative curve (DTG) is shown in Figure 3B. Apart from that, the main results are summarized in Table 2. The initial degradation temperature (T_I) for PLA pure was 303.7 °C, and the final degradation temperature, relative to 98% of loss mass, occurred at 377 °C, as expected [27]. PLA/MMT–Ct3% showed $T_I = 320.7$ °C, representing an increase of 7 °C. It is possible to assume that the MMT changed the crystalline structure of PLA and performed as a thermal protector of Ct essential oil once Ct has a volatilization temperature of approximately 200 °C [28]. While the samples PLA/MMT–Ct10%, PLA/MMT–Ct15%, and PLA/MMT–Ct20% had random T_I values, which suggests that the Ct oil is in excess, Ct oil playing the role of a plasticizing agent instead of being trapped between MMT lamellae.

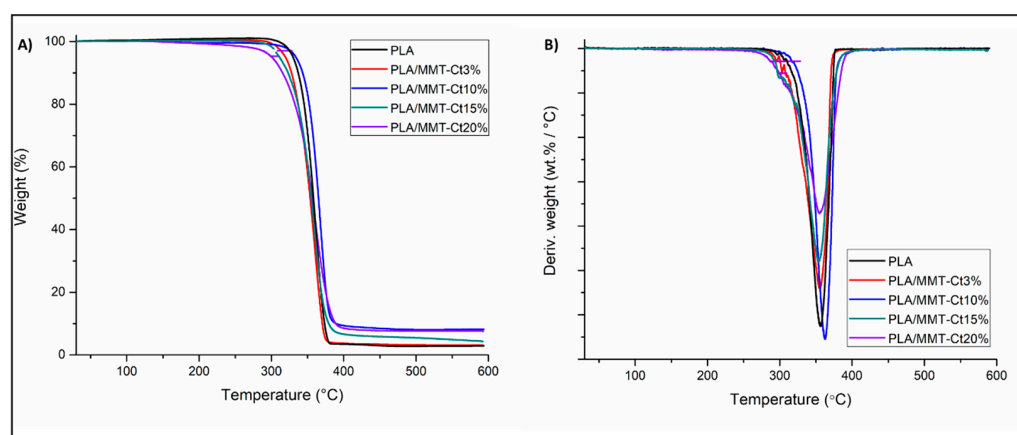


Figure 3. TGA (A) and DTG (B) curves of PLA; PLA/MMT–Ct3%; PLA/MMT–Ct10%; PLA/MMT–Ct15% and PLA/MMT–Ct20%.

Therefore, the results obtained for PLA/MMT–Ct composites are satisfactory since MMT was used as a carrier of Ct essential oil and was able to protect Ct from degrading processes during the composites processing thermally. In addition, both TGA results and XRD indicate the MMT interaction with PLA increased the crystallinity and the thermal properties. Similar interaction reports of polymers and Ct functional groups have been previously reported in the literature [29].

3.4. Differential Scanning Calorimetry

The effect of MMT–Ct incorporated in different amounts into the PLA matrix was analyzed using Differential Scanning Calorimetry (DSC), Figure 4A, where the melting point temperature (T_m) for crystallization was evaluated. From the DSC curves and cooling ramp, it was possible to analyze the crystallization temperature (T_c), as shown in Table 2 and Figure 4A. PLA/MMT–Ct3% results showed a slight increase in T_c compared to pure PLA. This result corroborates with the interpretation from TGA data, which suggest that MMT plays a nucleating role in the PLA matrix, enabling it to provide action by modifying the sizes and shapes of the crystals [30,31]. On the other hand, T_c values for the PLA/MMT–Ct10%, PLA/MMT–Ct15%, and PLA/MMT–Ct20% were 99.94 °C, 99.8 °C, and 97.34 °C, respectively, lower than the T_c of PLA pure, for which the value was 107.6 °C. The Ct essential oil probably is in excess in PLA samples, with a hybrid proportion higher than MMT–Ct10%, meaning more interaction with the polymeric sample, where the oil can play a role as a plasticizing agent. That was confirmed using the crystallinity degree (X_c) values, shown in Table 2. PLA/MMT–Ct10%, PLA/MMT–Ct15%, and PLA/MMT–Ct20% showed X_c of 2.86%, 3.12%, and 2.62%, respectively, against 3.11% of PLA crystallinity degree. This fact is attributed to the organic functional groups of Ct essential oils, which are possibly

acting with a plasticizing agent; that interaction with polymer is attributed to the alkyl radicals present probably because it is in excess in the PLA matrix [19].

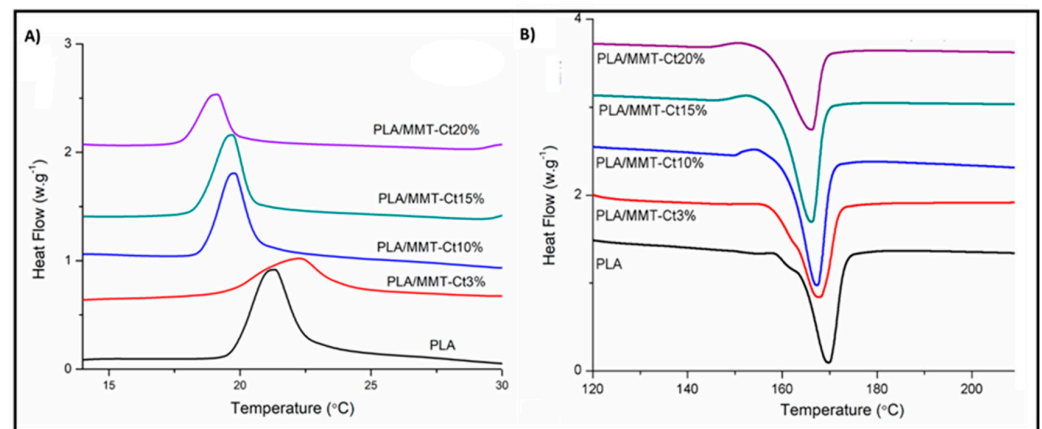


Figure 4. DSC-curves of PLA and composites: (A) cooling curves, (B) second heating curve.

Regarding the second DSC heating ramp, the PLA melting temperature (T_m) curve indicates the presence of two stereoisomers of PLA, L- and D-lactic acid. The L (levogyre) and D (dextrogyre) form due to their polarized light effect [32,33]. Thus, the DSC curves, presented in Table 2, show the T_m values for each lactic acid in one of the chiral molecules; the melting temperature (T_m) PLLA is between 130 and 180 °C and that for PDLA is between 190 and 230 °C [31]. Thus, the present PLA studied is characterized by the PLLA, indicating it to be a semicrystalline thermoplastic polyester polymer. It is possible to observe that the PLA and its composites showed that adding the hybrids did not cause a significant change.

3.5. Mechanical Tests

The mechanical tests were carried out to evaluate the samples' performance after MMT-Ct was incorporated and the effect of Ct essential oil into the polymeric matrix. Table 3 presents the mechanical results in terms of the modulus of elasticity (E), maximum elongation (ϵ_{max}), and tensile strength (σ_{rup}). From the obtained curves, it is possible to verify that pure PLA presents a fragile behavior compared to its composites. When MMT-Ct3% and MMT-Ct10% were added to the PLA, the composites showed higher elastic modulus values of 27.35 and 19.64 MPa, respectively; it indicates good dispersion of MMT into the polymeric matrix, and the Ct essential oil had a synergic effect. Furthermore, the literature reports that using clays acts as a reinforcing agent. A similar effect in mechanical properties of PLA was observed by Risyon et al., regarding the incorporation of halloysite (HNTs) into PLA; they reported good dispersion of halloysite in films of PLA when incorporated 1.5% and 3.0% by weight of HNTs, an event explained by an increase in hydrogen bonds between PLA and HNTs compared to films incorporated with higher concentrations of HNTs. The higher the number of hydrogen bonds provided strong films, which exhibited high tensile strength, Young's modulus, and yield strength, as the hydrogen bonds provided greater resistance to the forces applied to the films [34,35].

When the concentration of MMT-Ct in PLA increases, the composites start to behave more tenaciously, suggesting that Ct oil is saturated for concentrations MMT-Ct15% and MMT-Ct20%, where a pronounced increase in elongation at break is found, as shown in Table 3, due to the availability of oil to interact with the polymeric matrix as a plasticizer. Consequently, MMT-Ct15% and MMT-Ct20% showed reduced mechanical properties, elastic modulus, and tensile strength results. Similar results were observed by Dong Liu, in which polymeric matrices with a higher concentration of essential oil showed less tensile strength but a greater elongation at break compared to the polymer without the addition of essential oil [36]. In this way, adding essential oil reduced the interaction between the PLA

molecules and the chain-to-chain interactions of the polymer. As a result, this would cause a significant reduction in the tension of the films obtained from PLA/MMT-Ct.

Table 3. Mechanical properties: elastic modulus (E); tensile strength ($\epsilon_{\text{máx}}$); and elongation at break (σ_{rup}).

| Samples | Elastic Modulus (E) (MPa) | Tensile Strength (σ) (MPa) | Elongation at Break (ϵ) (%) |
|---------------|---------------------------|-------------------------------------|--|
| PLA | 15.4 \pm 3.4 | 28.5 \pm 8.3 | 10.4 \pm 3.2 |
| PLA/MMT-Ct3% | 27.3 \pm 7.0 | 34.8 \pm 1.9 | 3.5 \pm 0.7 |
| PLA/MMT-Ct10% | 19.6 \pm 8.2 | 43.5 \pm 38.0 | 13.0 \pm 5.9 |
| PLA/MMT-Ct15% | 10.7 \pm 2.1 | 18.9 \pm 2.7 | 48.3 \pm 24.2 |
| PLA/MMT-Ct20% | 5.9 \pm 1.5 | 11.1 \pm 2.6 | 43.7 \pm 33.4 |

3.6. Migration Test

Migration tests were performed to quantify the exudation effect of Ct oil from the composite's sample surface. For that, the weight of all samples was monitored up to 480 h (20 days), as shown in Figure 5. Through the proportionality law, it was determined that the quantities of oil that migrated to the surface of the composite in 480 h were 0.03%, 0.16%, 0.45%, 0.50%, and 2.08%, for samples PLA, PLA/MMT-Ct3%, PLA/MMT-Ct10%, PLA/MMT-Ct15%, and PLA/MMT-Ct20%, respectively. Both PLA/MMT-Ct15% and PLA/MMT-Ct20% have a release rate higher than that of the other samples with less content of Ct. High exudation rates were found for similar systems [37]. The lower concentration of Ct, sample PLA/MMT-Ct3%, shows an interesting characteristic, which was observed as a release only on the first day; it is reasonable to argue that almost all Ct is trapped between the MMT lamellae, so it is not available in the polymeric matrix surface to be identified by the exudation process. The results obtained from the migration test considering the thermal and mechanical analyses point out the saturation of Ct in the formulations PLA/MMT-Ct15% and PLA/MMT-Ct20%. Based on the results, the optimum concentration could be achieved between 3% and 10% as it presents an intermediate loading with a controlled release over time; it is worth mentioning that the intermediate concentration showed a satisfactory value in its mechanical properties.

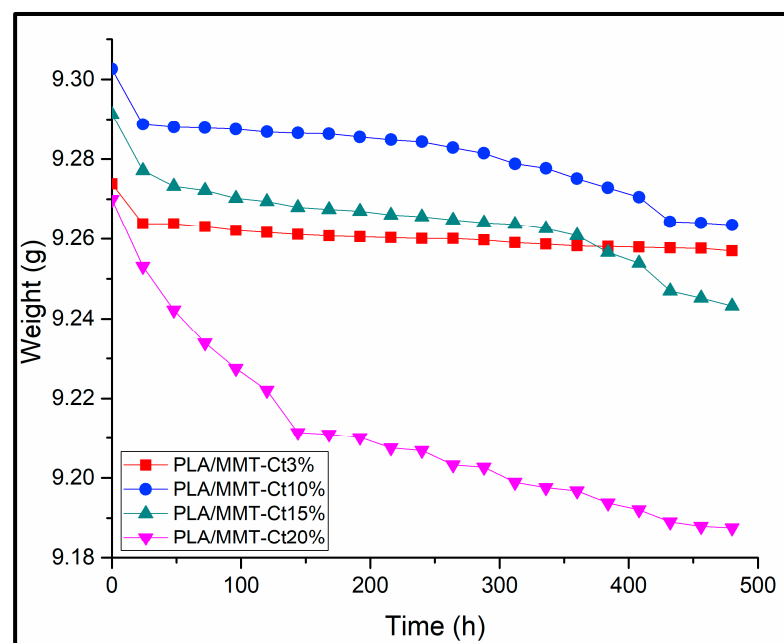


Figure 5. Migration graphs as a function of PLA time and nanocomposites.

Due to the nature of the compounds used, the chemical interaction between them is limited (as indicated by Fourier Transform Infrared Spectroscopy (FTIR) analyzes in previous studies demonstrating strong chemical interaction between the groups in the matrix and MMT) [38]. The main associated mechanism therefore resides in the encapsulation of the essential oil by the clay (with effective intercalation of the EOs in the clay, increasing the distance between the clay layers and highlighting the potential role of clay as a transporting agent) [15]. Thus, due to the volatile nature of the oil, it tends to exude (as demonstrated by the migration test), more directly impacting other properties such as material crystallinity and mechanical properties, depending on its concentration. It is important to point out that it was necessary to maintain the appropriate properties for the application of the material, something that would not be possible with the direct application of oil in the polymeric material.

4. Conclusions

The potential of PLA filled with montmorillonite (MMT)–citronella essential oil (Ct) hybrid, PLA/MMT–Ct, in different amounts was evaluated as an active film for packaging marketing, suitable to release Ct as an antimicrobial agent. The MMT–Ct hybrid was incorporated into the PLA matrix with different concentrations of 3, 10, 15, and 20 wt%. XRD results showed an increase in the interlayer of MMT when Ct was incorporated, even in lower concentration, meaning that Ct was trapped between the MMT lamellae, a great result once the MMT was used to play a role as a carrier and thermal protector of Ct, promoting a composite material suitable for industrial processing, as extrusion. The micrographs obtained using SEM showed a rougher surface with homogeneous distribution when MMT–Ct was incorporated in different amounts, suggesting good dispersion of MMT. According to TGA data, samples with a higher concentration of hybrid, PLA/MMT–Ct15% and PLA/MMT–Ct20% showed less thermal stability. Moreover, DSC results evidenced a reduction in T_c temperature and lower crystalline degree compared to the PLA matrix. Mechanical tests were the key to prove that the hybrid MMT–Ct15% and PLA/MMT–Ct20% were in excess in the matrix polymeric once it showed an increase in elongation at break and reduction in the maximum tensile strength. From that, it is possible to assert that Ct, in excess, can interact more with a polymeric matrix playing a role as a plasticizing agent, providing a more amorphous and ductile material. The migration tests demonstrated a higher release rate of Ct oil from PLA–MMT15% and PLA–MMT20% composite films. In short, the results obtained from the migration test as thermal and mechanical analyses point out the saturation of Ct in the formulations PLA/MMT–Ct15% and PLA/MMT–Ct20%. Therefore, this work suggests a range of optimum concentrations, between MMT–Ct3% and MMT–Ct10%, that present the best release relation and showed suitable value in its mechanical properties. The antimicrobial effectiveness of PLA/MMT with different amounts of Ct is a limitation of the present study, an issue to be explored in subsequent studies. However, the effective migration of Ct from the film is promising since active packaging must have a substance that migrates to the food, providing a protective barrier against microorganisms, which points out the potential of developed film for active film formulations.

Author Contributions: Conceptualization, R.R.F., R.F.S.T.; methodology, R.R.F., M.C.F., A.M., R.F.S.T.; validation, R.R.F., M.C.F., R.F.S.T.; formal analysis, R.R.F., M.C.F., A.M., R.F.S.T.; investigation, R.R.F., M.C.F., A.M., R.F.S.T.; resources, R.F.S.T.; data curation, R.R.F., M.C.F., A.M., R.F.S.T., writing-original draft, R.R.F., R.F.S.T.; writing-review and editing, R.R.F., R.F.S.T.; supervision, R.F.S.T.; project administration, R.F.S.T.; funding acquisition, R.F.S.T.; All authors have read and agreed to the published version of the manuscript.

Funding: This research was funded by Fundação de Amparo à Pesquisa do Estado de São Paulo (2018/06732-7).

Institutional Review Board Statement: Not applicable.

Informed Consent Statement: Not Applicable.

Data Availability Statement: The data presented in this study are available on request from the corresponding author. The data are not publicly available due to an ongoing study.

Acknowledgments: The authors thank the FATEC-Mauá, UFABC, and SENAI Mario Amato.

Conflicts of Interest: The authors declare no conflict of interest.

References

1. Madhumitha, G.; Fowsiya, J.; Roopan, S.M.; Thakur, V.K. Recent advances in starch–clay nanocomposites. *Int. J. Polym. Anal. Charact.* **2018**, *23*, 331–345. [[CrossRef](#)]
2. Kargarzadeh, H.; Huang, J.; Lin, N.; Ahmad, I.; Mariano, M.; Dufresne, A.; Thomas, S.; Gał, A. Recent developments in nanocellulose-based biodegradable polymers, thermoplastic polymers, and porous nanocomposites. *Prog. Polym. Sci.* **2018**, *87*, 197–227. [[CrossRef](#)]
3. Ferreira, F.V.; Dufresne, A.; Pinheiro, I.F.; Souza, D.H.S.; Gouveia, R.F.; Mei, L.H.I.; Lona, L.M.F. How do cellulose nanocrystals affect the overall properties of biodegradable polymer nanocomposites: A comprehensive review. *Eur. Polym. J.* **2018**, *108*, 274–285. [[CrossRef](#)]
4. Ainali, N.M.; Kalaronis, D.; Evgenidou, E.; Kyzas, G.Z.; Bobori, D.C.; Kaloyianni, M.; Yang, X.; Bikiaris, D.N.; Lambropoulou, D.A. Do poly(lactic acid) microplastics instigate a threat? A perception for their dynamic towards environmental pollution and toxicity. *Sci. Total Environ.* **2022**, *832*, 155014. [[CrossRef](#)]
5. Sadeghi, A.; Razavi, S.M.A.; Shaharampour, D. Fabrication and characterization of biodegradable active films with modified morphology based on polycaprolactone-poly(lactic acid)-green tea extract. *Int. J. Biol. Macromol.* **2022**, *205*, 341–356. [[CrossRef](#)]
6. Ma, Y.; Li, L.; Wang, Y. Development of PLA-PHB-based biodegradable active packaging and its application to salmon. *Packag. Technol. Sci.* **2018**, *31*, 739–746. [[CrossRef](#)]
7. Zheng, H.; Tang, H.; Yang, C.; Chen, J.; Wang, L.; Dong, Q.; Shi, W.; Li, L.; Liu, Y. Evaluation of the slow-release poly(lactic acid)/poly(hydroxyalkanoates) active film containing oregano essential oil on the quality and flavor of chilled pufferfish (*Takifugu obscurus*) filets. *Food Chem.* **2022**, *385*, 132693. [[CrossRef](#)]
8. Bai, T.; Zhu, B.; Liu, H.; Wang, Y.; Song, G.; Liu, C.; Shen, C. Biodegradable poly(lactic acid) nanocomposites reinforced and toughened by carbon nanotubes/clay hybrids. *Int. J. Biol. Macromol.* **2020**, *151*, 628–634. [[CrossRef](#)]
9. Alves, J.L.; Rosa, P.d.T.V.; Realinho, V.; Antunes, M.; Velasco, J.I.; Morales, A.R. The effect of Brazilian organic-modified montmorillonites on the thermal stability and fire performance of organoclay-filled PLA nanocomposites. *Appl. Clay Sci.* **2020**, *194*, 105697. [[CrossRef](#)]
10. Abdallah, W.; Mirzadeh, A.; Tan, V.; Kamal, M.R. Influence of Nanoparticle Pretreatment on the Thermal, Rheological and Mechanical Properties of PLA-PBSA Nanocomposites Incorporating Cellulose Nanocrystals or Montmorillonite. *Nanomaterials* **2018**, *9*, 29. [[CrossRef](#)]
11. Nonato, R.C.; Mei, L.H.I.; Bonse, B.C.; Chinaglia, E.F.; Morales, A.R. Nanocomposites of PLA containing ZnO nanofibers made by solvent cast 3D printing: Production and characterization. *Eur. Polym. J.* **2019**, *114*, 271–278. [[CrossRef](#)]
12. Zhang, S.; Chen, J.; Yin, X.; Wang, X.; Qiu, B.; Zhu, L.; Lin, Q. Microencapsulation of tea tree oil by spray-drying with methyl cellulose as the emulsifier and wall material together with chitosan/alginate. *J. Appl. Polym. Sci.* **2017**, *134*, 1–10. [[CrossRef](#)]
13. Inkinen, S.; Hakkarainen, M.; Albertsson, A.C.; Södergård, A. From lactic acid to poly(lactic acid) (PLA): Characterization and analysis of PLA and Its precursors. *Biomacromolecules* **2011**, *12*, 523–532. [[CrossRef](#)] [[PubMed](#)]
14. Dhatarwal, P.; Sengwa, R.J.; Choudhary, S. Effect of intercalated and exfoliated montmorillonite clay on the structural, dielectric and electrical properties of plasticized nanocomposite solid polymer electrolytes. *Compos. Commun.* **2017**, *5*, 1–7. [[CrossRef](#)]
15. Torin, R.F.S.; Camani, P.H.; da Silva, L.N.; Sato, J.A.P.; Ferreira, F.F.; Rosa, D.d.S. Effect of clay and clay/essential oil in packaging films. *Polym. Compos.* **2018**, *39*, 4034–4040. [[CrossRef](#)]
16. Kyung, E.G.; Song, B. Effect of java citronella essential oil addition on the physicochemical properties of Gelidium corneum-chitosan composite films. *Food Sci. Biotechnol.* **2020**, *29*, 909–915. [[CrossRef](#)]
17. Wang, L.; He, J.; Zhu, L.; Wang, Y.; Feng, X.; Chang, B.; Karahan, H.E.; Chen, Y. Assembly of pi-functionalized quaternary ammonium compounds with graphene hydrogel for efficient water disinfection. *J. Colloid Interface Sci.* **2019**, *535*, 149–158. [[CrossRef](#)]
18. Ojagh, S.M.; Ghorbani, M.; Hasani, M.; Resources, N.; Resources, N.; Resources, N.; Branch, S.; Azad, I. Nano-Encapsulation of Lemon Essential Oil Approach to Reducing the Oxidation Process in Fish Burger during Refrigerated Storage. *J. Food Biosci. Technol.* **2020**, *10*, 35–46.
19. Yahyaoui, M.; Gordobil, O.; Herrera Díaz, R.; Abderrabba, M.; Labidi, J. Development of novel antimicrobial films based on poly(lactic acid) and essential oils. *React. Funct. Polym.* **2016**, *109*, 1–8. [[CrossRef](#)]
20. Park, K.; Sadeghi, K.; Panda, P.K.; Seo, J.; Seo, J. Ethylene vinyl acetate/low-density polyethylene/oyster shell powder composite films: Preparation, characterization, and antimicrobial properties for biomedical applications. *J. Taiwan Inst. Chem. Eng.* **2022**, *134*, 104301. [[CrossRef](#)]
21. Pereira, R.B.; Morales, A.R. Estudo do comportamento térmico e mecânico do PLA modificado com aditivo nucleante e modificador de impacto TT—Study of mechanical and thermal behavior of PLA modified with nucleating additive and impact modifier. *Polímeros* **2014**, *24*, 198–202. [[CrossRef](#)]

22. Rhim, J.W.; Hong, S.I.; Ha, C.S. Tensile, water vapor barrier and antimicrobial properties of PLA/nanoclay composite films. *LWT Food Sci. Technol.* **2009**, *42*, 612–617. [[CrossRef](#)]
23. Abdelwahab, M.A.; Flynn, A.; Chiou, B.S.; Imam, S.; Orts, W.; Chiellini, E. Thermal, mechanical and morphological characterization of plasticized PLA-PHB blends. *Polym. Degrad. Stab.* **2012**, *97*, 1822–1828. [[CrossRef](#)]
24. Palsikowski, P.A.; Kuchnier, C.N.; Pinheiro, I.F.; Morales, A.R. Biodegradation in Soil of PLA/PBAT Blends Compatibilized with Chain Extender. *J. Polym. Environ.* **2018**, *26*, 330–341. [[CrossRef](#)]
25. Ramesh, P.; Prasad, B.D.; Narayana, K.L. Effect of fiber hybridization and montmorillonite clay on properties of treated kenaf/ aloe vera fiber reinforced PLA hybrid nanobiocomposite. *Cellulose* **2020**, *27*, 6977–6993. [[CrossRef](#)]
26. Shojaee-Aliabadi, S.; Mohammadifar, M.A.; Hosseini, H.; Mohammadi, A.; Ghasemlou, M.; Hosseini, S.M.; Haghshenas, M.; Khaksar, R. Characterization of nanobiocomposite kappa-carrageenan film with Zataria multiflora essential oil and nanoclay. *Int. J. Biol. Macromol.* **2014**, *69*, 282–289. [[CrossRef](#)] [[PubMed](#)]
27. de Macedo, J.R.N.; dos Santos Rosa, D. Effect of Fiber and Starch Incorporation in Biodegradation of PLA-TPS-Cotton Composites. *Key Eng. Mater.* **2015**, *668*, 54–62. [[CrossRef](#)]
28. El Asbahani, A.; Miladi, K.; Badri, W.; Sala, M.; Addi, E.H.A.; Casabianca, H.; El Mousadik, A.; Hartmann, D.; Jilale, A.; Renaud, F.N.R.; et al. Essential oils: From extraction to encapsulation. *Int. J. Pharm.* **2015**, *483*, 220–243. [[CrossRef](#)]
29. Shemesh, R.; Krepker, M.; Goldman, D.; Danin-Poleg, Y.; Kashi, Y.; Nitzan, N.; Vaxman, A.; Segal, E. Antibacterial and antifungal LDPE films for active packaging. *Polym. Adv. Technol.* **2015**, *26*, 110–116. [[CrossRef](#)]
30. Najafi, N.; Heuzey, M.C.; Carreau, P.J.; Wood-Adams, P.M. Control of thermal degradation of polylactide (PLA)-clay nanocomposites using chain extenders. *Polym. Degrad. Stab.* **2012**, *97*, 554–565. [[CrossRef](#)]
31. Zhao, H.; Cui, Z.; Wang, X.; Turng, L.S.; Peng, X. Processing and characterization of solid and microcellular poly(lactic acid)/polyhydroxybutyrate-valerate (PLA/PHBV) blends and PLA/PHBV/Clay nanocomposites. *Compos. Part B Eng.* **2013**, *51*, 79–91. [[CrossRef](#)]
32. Sun, J.; Yu, H.; Zhuang, X.; Chen, X.; Jing, X. Crystallization behavior of asymmetric PLLA/PDLA blends. *J. Phys. Chem. B* **2011**, *115*, 2864–2869. [[CrossRef](#)] [[PubMed](#)]
33. Rabelo, L.H.; Munhoz, R.A.; Marini, J.; Maestrelli, S.C. Development and characterization of PLA composites with high contents of a Brazilian refractory clay and improved fire performance. *Mater. Res.* **2022**, *25*. [[CrossRef](#)]
34. Risyon, N.P.; Othman, S.H.; Basha, R.K.; Talib, R.A. Characterization of polylactic acid/halloysite nanotubes bionanocomposite films for food packaging. *Food Packag. Shelf Life* **2020**, *23*, 100450. [[CrossRef](#)]
35. Kumar Panda, P.; Jebastine, J.; Ramarao, M.; Fairouz, S.; Reddy, C.K.; Nasif, O.; Alfarraj, S.; Manikandan, V.; Jenish, I. Exploration on Mechanical Behaviours of Hyacinth Fibre Particles Reinforced Polymer Matrix-Based Hybrid Composites for Electronic Applications. *Adv. Mater. Sci. Eng.* **2021**, *2021*, 4933450. [[CrossRef](#)]
36. Liu, D.; Li, H.; Jiang, L.; Chuan, Y.; Yuan, M.; Chen, H. Characterization of active packaging films made from poly(lactic acid)/poly(trimethylene carbonate) incorporated with oregano essential oil. *Molecules* **2016**, *21*, 695. [[CrossRef](#)]
37. Damascena, L.H.C.; Rosa, G.A.D.; Maia, A.; Derval, S.; Torin, R.F.S. Estudo da Interação e Migração dos Óleos Carvacrol e Eugenol Incorporados No Nanocompósito (PEBD/Nanoargila). 2017; Volume 3. Available online: <http://www.pos.cps.sp.gov.br/files/artigo/file/251/ee1ba3894243510bae73456fa389350c.pdf> (accessed on 1 November 2022).
38. de Souza, A.G.; Dos Santos, N.M.A.; Torin, R.F.S.; Santos, D.R. Synergic antimicrobial properties of Carvacrol essential oil and montmorillonite in biodegradable starch films. *Int. J. Biol. Macromol.* **2020**, *164*, 1737–1747. [[CrossRef](#)]

Disclaimer/Publisher’s Note: The statements, opinions and data contained in all publications are solely those of the individual author(s) and contributor(s) and not of MDPI and/or the editor(s). MDPI and/or the editor(s) disclaim responsibility for any injury to people or property resulting from any ideas, methods, instructions or products referred to in the content.